THE JOURNAL OF PHYSICAL CHEMISTRY B

ARTICLE

pubs.acs.org/JPCB

Recognition-Mediated Light-Up of Thiazole Orange with Cucurbit[8]uril: Exchange and Release by Chemical Stimuli

Jyotirmayee Mohanty,*[,†] Neha Thakur,[‡] Sharmistha Dutta Choudhury,[†] Nilotpal Barooah,[†] Haridas Pal,[†] and Achikanath C. Bhasikuttan*[,†]

[†]Radiation & Photochemistry Division and [‡]Analytical Chemistry Division, Bhabha Atomic Research Centre, Mumbai 400 085, India

Supporting Information

ABSTRACT: This article reports a convenient supramolecular strategy to construct fluorescent photoswitchable molecular assemblies between a macrocyclic host, cucurbit[8]uril (CB8), and a fluorogenic dye, thiazole orange (TO). The interaction mechanism and the stable stoichiometric host−guest arrangements have been claimed on the basis of the optical absorption, steady-state and time-resolved fluorescence lifetime and anisotropy measurements, and also the geometry optimization studies. The CB8 recognized TO in its 2:2 stoichiometry exhibited spectacular fluorescence enhancement of the order of 1700 fold, which is the largest directly determined value so far reported for a dye in an organic macrocyclic system. This prospective 2CB8:2TO assembly responded to selected chemical stimuli such as metal ions, adamantylamine, and tryptophan, providing different dissociation mechanisms and demonstrating a controlled exchange and release action desired with such noncovalently linked assemblies. Positively, considering the aqueous solubility and biocompatibility of the host−guest constituents, this methodology can evolve into a general approach to deliver and operate intracellularly functional molecular components under chemical/thermal/optical trigger control, especially for therapeutic applications.

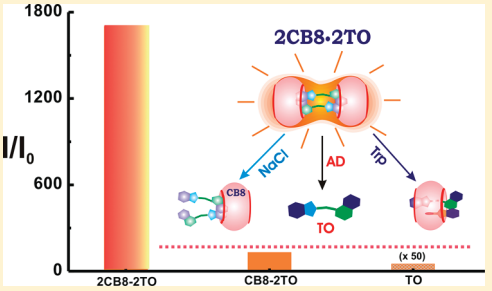

INTRODUCTION

Studies on recognition-mediated supramolecular assemblies have captured much attention over the past decade, as a large number of reports have demonstrated their direct application in fluorescence sensing,[1] on−off switches,[2,3] controlled drug uptake/release,[4,5] enzymatic assay,[6,7] nanocapsules,[8−10] photostabilization,[10−12] supramolecular catalysis,[13] supramolecular architectures,[14,15] and other stimulus-responsive functional devices.[4,8,10] These noncovalently held host−guest complexes are inherently dynamic in nature and highly selective for the complementary guests based on the various nonspecific and specific interactions and can be engineered to assemble and disassemble spontaneously in response to a range of stimuli.[4,6,8] This attribute provides a powerful strategy, which allows tuning of the host−guest assemblies to meet many of the desired functions, mentioned above.

Among the host of macrocycles, cucurbit[*n*]uril (CB*n*) homologues have received immense attention due to their versatile receptor properties, which can form stable inclusion complexes with small guest molecules such as organic dyes, metal cations, and protonated alkyl and arylamines.[10,16] CB*n* macrocycles consist of *n* glycoluril monomers joined by pairs of methylene bridges (Scheme 1) and have highly symmetrical structure with two identical carbonyl-laced portal ends. Though they possess hydrophobic cavities comparable to the well-known cyclodextrins (CDs), their guest binding features are distinctly different and are more attractive.[17,18] Apart from forming 1:1 stoichiometric complexes with varieties of cationic dyes, the higher homologues such as cucurbit[8]uril (CB8) are credited with forming higher stoichiometric (1:2 or 2:2) host−guest complexes by colocalizing π-stacked or charge transfer pairs in their cavities.[2,3,15,19,20] Such rigidized structural arrangements largely influence the excited state dynamics of the chromophoric guests, which are readily exploited for many technological applications.

In this context, studies on the radiatively responsive fluorogenic dyes, especially the cyanine dyes, have seen an increased research interest in recent years with main focus on their interaction with biomolecules as *optical DNA/RNA detectors* for their trace level detection[21,22] and therapeutic applications.[23,24] Among them, fluorescence behavior of an unsymmetrical dye, thiazole orange (TO, Scheme 1), is intriguing because of its remarkable environmentally sensitive emission quantum yields and extreme dimerization/aggregation tendencies.[22,25,26] TO is virtually nonfluorescent in aqueous solution ($\phi_f = 0.0002$) because of the highly efficient nonradiatively coupled photoisomerization and torsional motion between the benzthiazole and quinoline heterocycles.[22,25,26] However, in viscous solutions or on interaction with nucleobases, it displays substantial enhancement (>100-fold) in its emission yield, marking it as a *fluorogenic sensor* that reports on the local viscosity of its environment.[22] Moreover, TO has higher affinity toward tumor

Received: October 31, 2011
Revised: November 17, 2011
Published: December 01, 2011

Scheme 1. Structures of CB8, TO, and the CB8−TO Complexes[a]

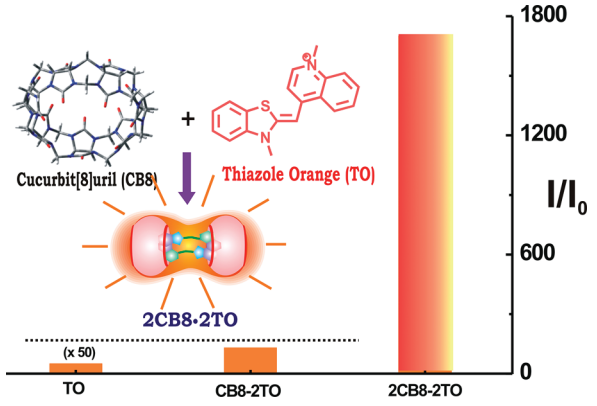

[a] The graph shows the emission intensity enhancement in TO for different stoichiometries.

cells than toward normal cells, which is useful for the early stage labeling of the cancer cells. TO and other cyanine dyes have also been applied to photoinactivate several model viruses and pathogens in RBCs, under conditions that produce limited hemolysis without the addition of quenchers or competitive inhibitors.[24]

Spectroscopically, the dimerization/aggregation has a strong effect on the electronic absorption and emission spectra of TO, which displays distinct spectral features depending on the monomer−dimer availability and often poses practical difficulties in trace level quantification.[25,27] This led to several studies to explore the dynamic states of the dye molecule, which exhibits vast changes in the molecular properties, by introducing supramolecular interactions with organized assemblies such as micelles and reverse micelles[28] or cavitand macrocycles such as calixarenes,[25] cyclodextrins.[28] On the other hand, employing the aforementioned cucurbituril macrocycles, we have reported the complexation and photophysical behavior of a number of technologically and biologically important fluorescent dyes,[10] e.g., rhodamines, triphenylmethane dyes, phenazine dyes, thioflavin T, projecting their applications as on−off systems,[3] molecular capsules,[8,9] water-based dye lasers,[10,11] etc. Here, the torsionally responsive TO dye provides an apt structural model, which is sensitive to molecular rigidization through noncovalent interaction revealing intriguing photophysics,[22,29] that can be explored for its potential utilities. Herein, we report spectacular light-up (fluorescence enhancement of the order of 1700 fold) of TO on its interaction with CB8. The recognition-mediated supramolecular complex is judiciously tuned by introducing selected release-stimulants to demonstrate the controlled release of the chromophoric dye from the host−guest assembly, a strategy which finds use in drug binding and release, sensing, and fluorescence on−off systems. During the preparation of this manuscript, Pang et al. have reported the formation of linear supramolecular polymers that is based on host−guest assembly of CB7/8 with TO in water.[30] While they carried out the studies at higher (∼50 μM) and lower (∼5 μM) TO concentrations, which mainly focused on the linear polymer formation, a detailed study on the photophysical features of the CB8−TO complex and the remarkable fluorescence enhancement in the complex at lower TO/CB8 ratio remained unexplored, which are mainly addressed here.

EXPERIMENTAL SECTION

Thiazole orange {1-methyl-4-[(3-methyl-2(3*H*)-benzothiazolylidene)methyl]quinolinium *p*-tosylate; TO}, cucurbit[8]uril (CB8), and 1-amantadine hydrochloride (adamantyl amine; AD) were obtained from Sigma-Aldrich and were used as received. Considering the low binding constant value (K_{salt} ∼ 100 M^{-1})[31] for the salt binding to the cucurbituril portals, the possibility of a trace amount of salts in the commercial CB8 sample has been neglected. Nanopure water (Millipore Gradient A10 System; conductivity of 0.06 μS cm^{-1}) was used to prepare the sample solutions. Ground-state optical absorption spectra were recorded using a Shimadzu model 160A UV−vis spectrophotometer (Tokyo, Japan). Steady-state fluorescence spectra were recorded using a Hitachi (Tokyo, Japan) model F-4500 spectrofluorimeter. The samples were excited at 465 nm to maintain minimum change in the absorbance, and changes, if any, have been normalized. Time-resolved fluorescence measurements were carried out using a time-correlated single-photon-counting (TCSPC) spectrometer (IBH, UK). In the present work, 445 nm diode laser (∼100 ps, 1 MHz repetition rate) was used as the excitation source, and a microchannel plate photomultiplier tube (MCP PMT) was used for fluorescence detection. A reconvolution procedure was used to analyze the observed decays using a proper instrument response function obtained by substituting the sample cell with a light scatterer (turbid solution of TiO_2 nanoparticles in water). With the present setup, the instrument time resolution is adjudged to be better than 50 ps. The fluorescence decays were analyzed as a sum of exponentials as,[32]

$$I(t) = \sum_i B_i \exp(-t/\tau_i) \quad (1)$$

where $I(t)$ is the time-dependent fluorescence intensity and B_i and τ_i are the pre-exponential factor and the fluorescence lifetime for the ith component of the fluorescence decay, respectively. The quality of the fits and consequently the mono- or biexponential natures of the decays were judged by the reduced chi-square (χ^2) values and the distribution of the weighted residuals among the data channels. For a good fit, the χ^2 value was close to unity, and the weighted residuals were distributed randomly around zero among the data channels.[32]

For anisotropy measurements, samples were excited with a vertically polarized excitation beam, and the vertically and horizontally polarized fluorescence decays were collected with a large spectral bandwidth of ∼32 nm. Using these polarized fluorescence decays, the anisotropy decay function, $r(t)$, was constructed as follows:[32]

$$r(t) = \frac{I_V(t) - GI_H(t)}{I_V(t) + 2GI_H(t)} \quad (2)$$

$I_V(t)$ and $I_H(t)$ are the vertically and horizontally polarized decays, respectively, and G is the correction factor for the polarization bias of the detection setup. The G factor was determined independently by using a horizontally polarized excitation beam and measuring the two perpendicularly polarized fluorescence decays; measurements were repeated three times. The geometry optimization calculations were performed with Gausian 92 suite of package at PM3 (MM) level, without any solvent consideration.[33]

dx.doi.org/10.1021/jp210432t |*J. Phys. Chem. B* 2012, 116, 130–135

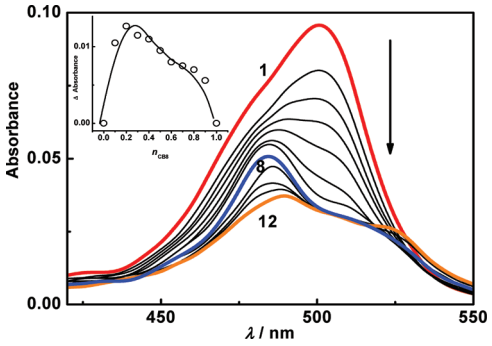

Figure 1. Absorption spectra of Thiazole Orange (~3 μM) in water with varying concentrations of [CB8]/μM: 0 (**1**); 0.04 (**2**); 0.12 (**3**); 0.2 (**4**); 0.32 (**5**); 0.56 (**6**); 1.2 (**7**); 2.0 (**8**); 5.0 (**9**); 10.0 (**10**); 25.0 (**11**), and 42.0 (**12**). Inset: Plot of absorbance at 480 nm with change in mole fraction of CB8 recorded from a solution containing TO, CB8, and 1 M NaCl, following Jobs plot method.

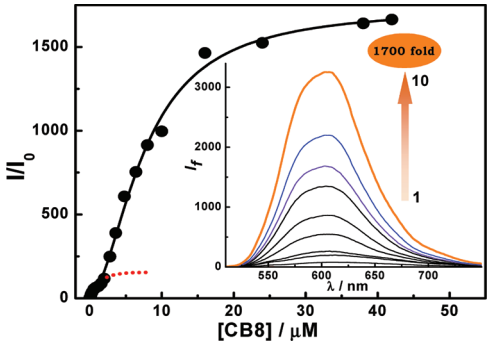

Figure 2. Changes in the fluorescence intensity of ~3 μM of TO with increasing concentration of CB8, plotted relative to that of free dye (I/I_0). λ_{ex} = 465 nm, λ_{mon} = 605 nm. The dotted and solid lines are the 1:2 binding saturation and the fitted curve for the 2:2 complex formation, respectively, as detailed in Note 1, Supporting Information. Inset: Fluorescence spectral changes recorded from TO solution (3 μM) with CB8/μM: 0 (**1**); 42 (**10**). λ_{ex} = 465 nm.

RESULTS AND DISCUSSION

The monomer, H-dimer, and higher H-aggregates of TO display distinct electronic states with absorption maxima around 500, 470, and 430 nm, respectively.[25,27] In the present study, a ~3 μM aqueous solution of TO displayed an absorption maximum at 500 nm with a shoulder at ~475 nm, in good agreement with the reported values (Figure 1).[25,27] Incremental addition of CB8 to the TO solution resulted in the gradual decrease in the absorbance, prominently in the red side of the spectrum (up to ~2 μM CB8), while the shoulder band at the blue edge resolved into a new band with a maximum at ~485 nm, leaving the 500 nm band as a shoulder similar to the reported spectrum of TO dimer, as shown in Figure 1. However, beyond this host concentration and until ~40 μM CB8, the spectrum again shifted bathochromically by ~10 nm, registering a new broad absorption profile with a maximum at 495 nm and a shoulder at ~525 nm (Figure 1). Because CB8 does not have any absorption in the region monitored, clearly the changes observed in the spectral features are related to the interaction of TO with the CB8 macrocycle. Moreover, the changes in the spectral features of TO seen at different concentration ranges of CB8 (less than and more than 2 μM CB8) also point to the existence of more than one host−guest equilibrium with change in the host concentration.

The CB8-induced changes in the absorption profiles of TO were also corroborated by the emission measurements. Strikingly, as presented in the inset of Figure 2, the addition of CB8 resulted in a dramatic enhancement in the emission intensity of TO, showing a broad spectral profile centered at ~605 nm, which otherwise is nearly nonemissive.[25,26] A comparison with the intensity at 605 nm in the absence of CB8, the overall fluorescence enhancement is evaluated to be 1700 ± 100 fold, attained in the presence of ~40 μM of CB8. Though emission enhancement of the order of more than 1000 fold is known for TO on binding with biomolecules,[34] the 1700 fold enhancement revealed here is the largest directly determined value so far reported for a dye in an organic macrocyclic system.

Note that earlier studies with different guest dye molecules showed emission quenching due to the colocalization of the guests within the CB8 cavity,[20] except the thioflavin T (ThT) dye, which displayed a dramatic spectral shift and enhancement due to the formation of an excimer complex within the CB8 cavity.[3] In the present system, apart from the clear signatures for dimeric TO seen in the absorption studies, excitation at different absorption wavelengths also confirmed that the fluorescence emission band in the CB8−TO system remained centered at ~605 nm, confirming the absence of monomers or higher aggregates of the dye (emission bands at 528 and 650 nm, respectively) in the system.[22,25] In a separate experiment, the excitation and emission spectra recorded for the dye alone at very high concentration, where the dimer formation is reported,[26] resembled to a large extent the features displayed by TO upon CB8 interaction.

Figure 2 shows the extent of fluorescence enhancement at 605 nm on addition of CB8 plotted relative to that of the free dye (I/I_0). A close look at the initial region reveals a quasisaturation at ~2 μM CB8 with an enhancement of ~130 fold, indicating an early stage complexation equilibrium. However, with higher concentrations of CB8, the emission intensity gets saturated with an overall fluorescence enhancement of ~1700 fold. Because, from the onset of titration itself (i.e., at higher TO/CB8 ratio), the absorption and emission spectra closely correspond to that of TO dimer, we believe that by virtue of large cavity size and high negative charge density at the portals, CB8 recognizes two TO molecules to exist in a 1:2 (CB8·TO) stoichiometric complex, represented by the quasisaturation in the initial region. Thereafter, on increasing the concentration of CB8, the 1:2 equilibrium gets shifted to a 2:2 assembly with spectacular enhancement in the TO fluorescence by ~1700-fold. Large enhancement in the radiative properties of such molecular rotor molecule is genuinely expected as the cucurbituril binding interaction would arrest the otherwise highly effective nonradiative relaxation channels, such as excited state torsional motion and photoisomerization process, very effectively.[22,25] In the case of the dimer complex, in addition to the increased molecular rigidity imparted by two CB8 moieties on the TO dimer (Scheme 1) the interactions among the colocalized TOs also play a pronounced role in modulating the properties of the complex. The contended stoichiometric shift from 1:2 complex to 2:2 complex with an increase in the CB8 concentration is also clearly reflected by the changes in the absorption maxima, which are highlighted in spectra 8 and 12, respectively, of Figure 1.

The modulation in the radiative properties of TO on interaction with CB8 was clearly seen from the significant increase in its

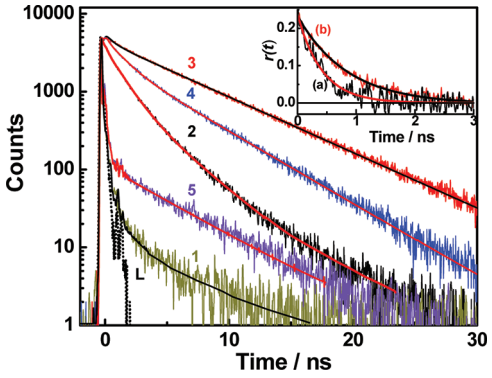

Figure 3. Fluorescence decay traces recorded for TO (~3 μM) at 605 nm on excitation at 445 nm, having CB8: 0 (**1**); 4 μM (**2**); 42 μM (**3**); 42 μM with 1 M NaCl (**4**); 42 μM with 500 μM tryptophan (**5**) (see Table S1 in Supporting Information for the time constants). Inset: Anisotropy decay curves measured at 605 nm for TO in the presence of CB8 in water, λ_{ex} = 445 nm. [CB8]: 0.5 μm (a) and 42.0 μM (b).

excited-state lifetime values as documented in the fluorescence decay profiles presented in Figure 3. Unlike the very short excited-state lifetime of TO monomer, which is only on the order of a few picoseconds for the free dye in aqueous solution,[29] the decay trace recorded at 605 nm (corresponding to the dimer emission) also displayed a much weaker long component (~2.5 ns) along with the fast component, which is within the resolution of the time-correlated single-photon-counting (TCSPC) instrument used here. However, the decay became clearly measurable in the presence of CB8, as the 1:2 complex displayed a triexponential decay having significant contributions from faster decay components (0.6 ns (15%), 1.8 ns (38%)) along with a slower decay component of lifetime ~5.7 ns (47%). See that for the proposed 2:2 complex, the decay kinetics became nearly single exponential, having >95% of ~5.7 ns component and manifesting severe retardation of the excited-state nonradiative relaxation channels, hence increasing its lifetime (Table S1). Moreover, the existence of the 1:2 and 2:2 assemblies were convincingly demonstrated in the rotational correlation time, τ_r, evaluated by the fluorescence anisotropy measurements. At the corresponding solution conditions for the 1:2 and 2:2 (CB8:TO) stoichiometries, the anisotropy decay provided τ_r as 500 ± 30 ps and 860 ± 50 ps for the respective samples (Figure 3 inset), which are further analyzed with Stokes−Einstein relationship:[3,18]

$$\tau_r = \frac{1}{6D_r} \text{ where } D_r = \frac{RT}{6V\eta}$$

Here, D_r and η are the rotational diffusion coefficient and viscosity of the medium, respectively, V is the hydrodynamic molecular volume of the complex, and T is the absolute temperature. By using the above relation, the evaluated effective hydrodynamic diameters of the complexes displayed an increase from 16.4 Å for the 1:2 complex to 19.7 Å for the 2:2 complex and is expected because of the addition of a second CB8 on TO. Geometry optimization at the PM3 (MM) level provided energy-minimized CB8·TO structures, both in the 1:2 and 2:2 geometries, as in Figure 4, having heat of formation (ΔH_f) values about −31 kcal/mol and −52 kcal/mol, respectively (also see Figure S1). Here, rather than encapsulating the dye in the CB8 cavity, the strong hydrogen bonding interactions at the portal regions

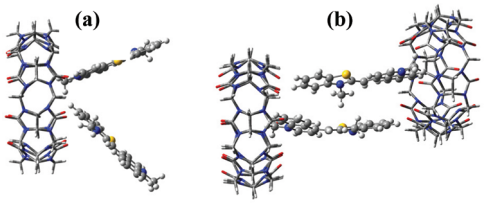

Figure 4. Geometry-optimized structures of 1:2 (a) and 2:2 (b) CB8:TO complexes obtained from PM3 (MM) level optimization using Gaussian package.

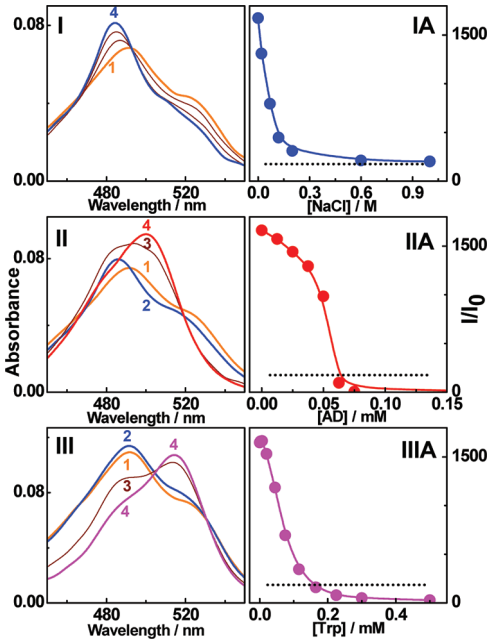

Figure 5. (I−III) Absorption spectral changes in a solution of TO (~3 μM) and CB8 (40 μM) with varying concentrations of stimulants: (I) [NaCl]/M; 0 (1); 0.02 (2); 0.07 (3); 1 (4). (II) [AD]/μM; 0(1); 50 (2); 75 (3); 500 (4). (III) [Trp]/μM; 0 (1); 2.5 (2); 165 (3); 500 (4). (IA−IIIA) Emission intensity changes at 600 nm for TO with NaCl (IA); AD (IIA); Trp (IIIA).

itself stabilizes the TO dimer in antiparallel arrangement which is more stable.[35]

In evaluating the binding constants from the curve in Figure 2, the presence of higher-order complexation equilibria, along with the monomer−dimer equilibrium, limits its quantitative estimation. However, considering the formation of 1:2 complexation, predominantly at lower concentration, and following the method discussed in Note 1 in Supporting Information, an approximate binding constant value, $K_{1:2} \sim 6 \times 10^{11}$ M^{-2} has been estimated. Similarly, at higher CB8 concentrations, assuming the conversion of 1:2 complexation to 2:2 complex, we determined the $K_{2:2}$ value as ~2×10^5 M^{-1} (Note 1, Supporting Information).[3]

Having demonstrated an efficient light-up of TO through the recognition-mediated 2:2 complex with CB8, our next aim was to introduce a release mechanism on demand for the entrapped guest to enable its projected applications (vide supra). In this context, we have employed different chemical additives such as metal ion (NaCl), tryptophan (Trp), or adamantylamine (AD) as stimuli, selected based on their biological importance and varying binding affinity toward CB8. The differential interactions

dx.doi.org/10.1021/jp210432t |J. Phys. Chem. B 2012, 116, 130–135

Scheme 2. Representation of the Interaction of Selected Chemical Stimuli Conveying Different Nonemissive Complexes and Providing Methods for Controlled Release Pathways

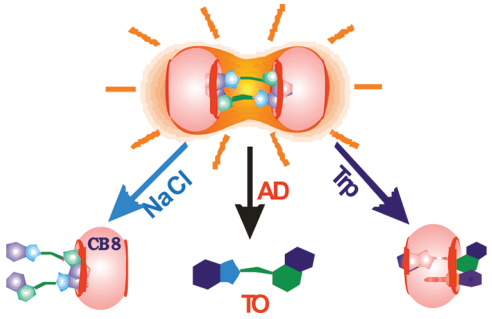

of these stimulants with the carbonyl portals, host cavity, or the included guest is expected to provide stoichiometric control desirably.

Absorption and emission measurements were carried out using the CB8·TO complex set for the maximum emission intensity (2:2 complex). On titration with NaCl, the emission intensity decreased drastically as shown in Figure 5 IA, signaling the disruption of the 2:2 complex due to the competitive interaction of Na^+ ions at the CB8 portals. At the same time, it is striking that the residual intensity remained at the level corresponding to the emission intensity of the 1:2 complex, even with 1 M salt (dotted lines, Figure 5IA). Concomitantly, the absorption spectra shifted slightly to the blue side along with hyperchromicity (Figure 5I), in good match with the changes expected for a 1:2 stoichiometry. These changes presented in Figure 5I is to be compared with the changes in Figure 1, in reverse. Confirmatory evidence for the partial release was seen from the Job's plot, evaluated in solutions of the 2:2 complex containing ~1 M salt, which displayed a maximum at ~0.33 mol fraction of CB8 corresponding to the 1:2 stoichiometry (inset of Figure 1). The decay profile recorded for the 2:2 complex in the presence of 1 M NaCl also showed a decreasing trend in the lifetime, toward a 1:2 complex as in Figure 3 (Table S1). Note that, because the competitive titrations involve multiple equilibria, the additional parameters introduced by the higher-order complexes make the fitting of competitive titrations a formidable task.

Next we used AD, a stronger CB8 binder which forms efficient inclusion complex with CB8.[36] Addition of ~100 μM of AD to the 2:2 fluorescent complex resulted in the complete decrease of the emission to that of free dye (Figure 5 IIA). Corroborating the complete rupture of the complex, the absorption spectrum also reverted completely to that of the monomer dye as presented in Figure 5II.

On the other hand, CB8 is recognized to form inclusion complexes with some of the amino acid residues, especially with Trp, highlighting its importance in detecting biomolecules.[15,19,37] With Trp as a stimulant, the 2:2 complex showed drastic decrease in the emission intensity, well below the 1:2 stoichiometric level (Figure 5 IIIA). However, the absorption spectrum, after attaining the spectral position of the 1:2 complex, evolved into a new band with the maximum ~14 nm red-shifted to the monomer peak (Figure 5III), which is quite distinct from the preceding two cases. From the emission intensity changes and the lifetime data (Figure 3), it has been adjudged that the spectral indications are due to the conversion of the CB8·2TO complex to a CB8·TO·Trp complex (Figure S1e). Essentially, it is likely that the TO−Trp charge transfer interaction within the CB8 cavity severely quenches the fluorescence emission. This process is evidently seen as a fast decay in the fluorescence profile as displayed in Figure 3, trace 5 (Table S1). The various stoichiometric complexes formed in the release pathway via chemical stimulants are schematically represented as in Scheme 2.

Apparently, the addition of the above chemical stimuli documents the switchover of a highly fluorescent 'on' state (or light-up) to a weakly fluorescent 'off' state, over a wide intensity range, compared to the other stoichiometric complexes feasible as highlighted in Scheme 1. Note that such recognition-mediated noncovalent binding and release strategy has found increasing demand in the present scenario, as several studies have demonstrated its application, especially in targeted drug delivery,[4,8,31] cellular activation of therapeutics,[4] detection of biomolecules,[15,19,37] enzymatic assays,[6,7] control of thermoresponsive properties of polymers,[36] molecular capsules,[8,9] on−off systems,[3] etc., all of which assert the convenience of designing the molecular assembly with apt molecular recognition partners for a specified function. Pertinently, this recognition-mediated binding and release strategy becomes meaningful for biological applications, as the cytotoxicity tests demonstrated that the constituent components are benign to the cellular ambience,[24,38] a positive note for therapeutic utility. Notably, the demonstration of polymeric assembly by Pang et al[30] adds one more dimension to the utility of such tunable molecular assemblies.

CONCLUSION

In conclusion, here we demonstrate a convenient molecular recognition approach to construct photochemically sensitive supramolecular assemblies of a macrocyclic host, cucurbit[8]uril (CB8) and a fluorogenic dye, thiazole orange (TO). The interaction mechanism and the stable stoichiomteric arrangements have been claimed on the basis of the optical absorption, steady-state and time-resolved fluorescence measurements, and also the geometry optimization studies. The remarkably high fluorescence response, which is of the order of 1700 fold, on the other hand, can be used indirectly for the trace level analysis of CB8 impurities even in the samples of CB homologues. Apart from the prominent modulation in the molecular properties of TO, the complex's response to selected stimuli, such as metal ions, adamantylamine, and tryptophan, demonstrated the controlled exchange and release action desired with such noncovalently linked assemblies for activation of dye/drug for the therapeutic uses. While the structure and active groups in the dye (guest) can be modified/tailored, such simple protocol leading to photoswitchable systems having aqueous solubility and biocompatibility can, in principle, evolve into a general strategy to deliver and operate intracellularly functional molecular components under chemical/optical/thermal trigger control. More studies in this perspective are being attempted.

ASSOCIATED CONTENT

Supporting Information. Additional figures, tables, and explanations. This material is available free of charge via the Internet at http://pubs.acs.org.

AUTHOR INFORMATION

Corresponding Authors

*E-mail: jyotim@barc.gov.in (J.M.); bkac@barc.gov.in (A.C.B.). Fax: (+) 22 25505151.

ACKNOWLEDGMENT

The authors acknowledge the encouragement and support provided by Dr. S. K. Sarkar, Head, RPCD, and Dr. T. Mukherjee, Director, Chemistry Group, BARC, during the studies.

REFERENCES

(1) (a) Dsouza, R. N.; Pischel, U.; Nau, W. M. *Chem. Rev.* **2011**, *111*, 7941–7980. (b) Chen, Y.; Liu, Y. *Chem. Soc. Rev.* **2010**, *39*, 495–505. (c) Bakirci, H.; Nau, W. M. *Adv. Funct. Mater.* **2006**, *16*, 237–242. (d) Wang, R.; Yuan, L.; Macartney, D. H. *Chem. Commun.* **2005**, 5867–5869.

(2) Wang, R.; Yuan, L.; Ihmels, H.; Macartney, D. H. *Chem.—Eur. J.* **2007**, *13*, 6468–6473.

(3) Mohanty, J.; Dutta Choudhury, S.; Upadhyaya, H. P.; Bhasikuttan, A. C.; Pal, H. *Chem.—Eur. J.* **2009**, *15*, 5215–5219.

(4) (a) Angelos, S.; Yang, Y.-W.; Patel, K.; Stoddart, J. F.; Zin, J. I. *Angew. Chem., Int. Ed.* **2008**, *47*, 2222–2226. (b) Kim, C.; Agasti, S. S.; Zhu, Z.; Isaacs, L.; Rotello, V. M. *Nature Chem.* **2010**, *2*, 962–966.

(5) Saleh, N.; Koner, A. L.; Nau, W. M. *Angew. Chem., Int. Ed.* **2008**, *47*, 5398–5401.

(6) Ghale, G.; Ramalingam, V.; Urbach, A. R.; Nau, W. M. *J. Am. Chem. Soc.* **2011**, *133*, 7528–7535.

(7) Hennig, A.; Bakirci, H.; Nau, W. M. *Nat. Methods* **2007**, *4*, 629–632.

(8) Dutta Choudhury, S.; Mohanty, J.; Pal, H.; Bhasikuttan, A. C. *J. Am. Chem. Soc.* **2010**, *132*, 1395–1401.

(9) Bhasikuttan, A. C.; Dutta Choudhury, S.; Pal, H.; Mohanty, J. *Isr. J. Chem.* **2011**, *51*, 634–645.

(10) Bhasikuttan, A. C.; Pal, H.; Mohanty, J. *Chem. Commun.* **2011**, *47*, 9959–9971.

(11) (a) Mohanty, J.; Jagtap, K.; Ray, A. K.; Nau, W. M.; Pal, H. *ChemPhysChem* **2010**, *11*, 3333–3338. (b) Mohanty, J.; Pal, H.; Ray, A. K.; Kumar, S.; Nau, W. M. *ChemPhysChem* **2007**, *8*, 54–56.

(12) (a) Koner, A. L.; Nau, W. M. *Supramol. Chem.* **2007**, *19*, 55–66. (b) Mohanty, J.; Nau, W. M. *Angew. Chem., Int. Ed.* **2005**, *44*, 3750–3754. (c) Nau, W. M.; Mohanty, J. *Int. J. Photoenergy* **2005**, *7*, 133–141.

(13) Pluth, M. D.; Bergman, R. G.; Raymond, K. N. *Science* **2007**, *316*, 85–88.

(14) (a) Frampton, M. J.; Anderson, H. L. *Angew. Chem., Int. Ed.* **2007**, *46*, 1028–1064. (b) Mohanty, J.; Bhasikuttan, A. C.; Dutta Choudhury, S.; Pal, H. *J. Phys. Chem. B* **2008**, *112*, 10782–10785.

(15) Ko, Y. H.; Kim, E.; Hwang, I.; Kim, K. *Chem. Commun.* **2007**, 1305–1315.

(16) (a) Lagona, J.; Mukhopadhyay, P.; Chakrabarti, S.; Isaacs, L. *Angew. Chem., Int. Ed.* **2005**, *44*, 4844–4870. (b) Lee, J. W.; Samal, S.; Selvapalam, N.; Kim, H.-J.; Kim, K. *Acc. Chem. Res.* **2003**, *36*, 621–630.

(17) (a) Jeon, W. S.; Moon, K.; Park, S. H.; Chun, H.; Ko, Y. H.; Lee, J. Y.; Lee, E. S.; Samal, S.; Selvapalam, N.; Rekharsky, M. V.; Sindelar, V.; Sobransingh, D.; Inoue, Y.; Kaifer, A. E.; Kim, K. *J. Am. Chem. Soc.* **2005**, *127*, 12984–12989. (b) Shaikh, M.; Mohanty, J.; Singh, P. K.; Nau, W. M.; Pal, H. *Photochem. Photobiol. Sci.* **2008**, *7*, 408–414. (c) Kandoth, N.; Dutta Choudhury, S.; Mohanty, J.; Bhasikuttan, A. C.; Pal, H. *J. Phys. Chem. B* **2010**, *114*, 2617–2626. (d) Dutta Choudhury, S.; Mohanty, J.; Bhasikuttan, A. C.; Pal, H. *J. Phys. Chem. B* **2010**, *114*, 10717–10727.

(18) Mohanty, J.; Bhasikuttan, A. C.; Nau, W. M.; Pal, H. *J. Phys. Chem. B* **2006**, *110*, 5132–5138.

(19) Ling, Y.; Wang, W.; Kaifer, A. E. *Chem. Commun.* **2007**, 610–612.

(20) Shaikh, M.; Dutta Choudhury, S.; Mohanty, J.; Bhasikuttan, A. C.; Pal, H. *Phys. Chem. Chem. Phys.* **2010**, *12*, 7050–7055.

(21) Jarikote, D. V.; Krebs, N.; Tannert, S.; Roder, B.; Seitz, O. *Chem.—Eur. J.* **2007**, *13*, 300–310.

(22) Silva, G. L.; Ediz, V.; Yaron, D.; Armitage, B. A. *J. Am. Chem. Soc.* **2007**, *129*, 5710–5718.

(23) (a) Rye, H. S.; Yue, S.; Wemmer, D. E.; Quesada, M. A.; Haugland, R. P.; Mathies, R. A.; Glazer, A. N. *Nucleic Acids Res.* **1992**, *20*, 2803–2812. (b) Kawakami, M.; Koya, K.; Ukai, Tatsuta, T.; N.; Ikegawa, A.; Ogawa, K.; Shishidi, T.; Chen, L. B. *J. Med. Chem.* **1998**, *41*, 130–142.

(24) Skripchenko, A.; Wagner, S. J.; Thompson-Montgomery, D.; Awatefe, H. *Transfusion* **2006**, *46*, 213–219.

(25) Lau, V.; Heyne, B. *Chem. Commun.* **2010**, *46*, 3595–3597.

(26) Nygren, J.; Svanvik, N.; Kubista, M. *Biopolymers* **1998**, *46*, 39–51.

(27) Nygren, J.; Andrade, J. M.; Kubista, M. *Anal. Chem.* **1996**, *68*, 1706–1710.

(28) Dutta Choudhury, S.; Bhasikuttan, A. C.; Pal, H.; Mohanty, J. *Langmuir* **2011**, *27*, 12312–12321.

(29) Karunakaran, V.; Lustres, J. L. P.; Zhao, L.; Ernsting, N. P.; Seitz, O. *J. Am. Chem. Soc.* **2006**, *128*, 2954–2962.

(30) Xu, Y.; Guo, M.; Li, X.; Malkovskiy, A.; Wesdemiotisa, C.; Pang, Y. *Chem. Commun.* **2011**, *47*, 8883–8885.

(31) Shaikh, M.; Mohanty, J.; Bhasikuttan, A. C.; Uzunova, V. D.; Nau, W. M.; Pal, H. *Chem. Commun.* **2008**, 3681–3683.

(32) Lakowicz, J. R. *Principles of fluorescence spectroscopy*; Springer: New York, 2006.

(33) Frisch, M. J.; Trucks, G. W.; Head-Gordon, M.; Gill, P. M. W.; Wong, M. W.; Foresman, J. B.; Johnson, B. G.; Schlegel, H. B.; Robb, M. A.; Replogle, E. S.; Gomperts, R.; Andres, J. L.; Raghavachari, K.; Binkley, J. S.; Gonzalez, C.; Martin, R. L.; Fox, D. J.; Defrees, D. J.; Baker, J.; Stewart, J. J. P.; Pople, J. A. *Gaussian 92, Revision E.1*, Gaussian, Inc., Pittsburgh, PA, 1992.

(34) Fei, X.; Gu, Y.; Ban, Y.; Liu, Z.; Zhang, B. *Bioorg. Med. Chem.* **2009**, *17*, 585–591.

(35) Biancardi, A.; Biver, T.; Marini, A.; Mennucci, B.; Secco, F. *Phys. Chem. Chem. Phys.* **2011**, *13*, 12595–12602.

(36) Rauwald, U.; Barrio, J.; Loh, X. J.; Scherman, O. A. *Chem. Commun.* **2011**, *47*, 6000–6002.

(37) Heitmann, L. M.; Taylor, A. B.; Hart, P. J.; Urbach, A. R. *J. Am. Chem. Soc.* **2006**, *128*, 12574–12581.

(38) Uzunova, V. D.; Cullinane, C.; Brix, K.; Nau, W. M.; Day, A. I. *Org. Biomol. Chem.* **2009**, *8*, 2037–2042.